

GUIDED-WAVE ACOUSTO-OPTICS FOR OPTICAL SIGNAL PROCESSING

V. M. N. Passaro

Dipartimento di Elettrotecnica ed Elettronica, Politecnico di Bari, ITALY
passaro@poliba.it

Abstract

In this invited paper some of very significant examples of guided-wave acousto-optical processors for optical signal processing and sensing applications are presented and summarized. Detailed performance comparisons with analogous electronic approaches are given, showing some advantages of using the guided-wave acousto-optic technology, in particular for space applications.

Introduction

Nowadays, Integrated Optics (I.O.) has definitely reached the technological maturity with a large number of applications on industrial scale. Among them, I.O. devices are expected to positively impact the space segment technology due to their intrinsic characteristics which make them attractive with respect to conventional electronic technologies, particularly using the Acousto-Optic (AO) technology.

It is known that AO technology can be used for a number of signal processing applications, such as data correlation and compression, time and space integration, Fourier transform, filtering and so on. Several very recent examples can be found in literature, as tunable filters [1], switches [2], delay lines [3].

Other significant research results have been also obtained in space applications for earth observation, telecommunications and radar surveillance [4-6]. In particular, research efforts have been focused on optical control processors and real-time correlators for 2D image reconstruction in Synthetic Aperture Radar (SAR) and beam steering in linearly active phased array antennas for beam forming networks (BFN). These devices are based on the performance of guided-wave non collinear AO interaction in linear Bragg cells driven by unidirectional interdigital transducers (IDT), and allow to fully exploit the high data parallelism connected with optical signal processing techniques. In fact, specific advantages have been demonstrated by using guided-wave AO devices over their electronic counterpart, mostly in space [6]:

- ◆ smaller size due to lower wavelengths involved means overall payload mass reduction and, then, both launch cost and satellite cost reduction;
- ◆ reduced losses, related to higher efficiency, lead to less power consumption, with a possible reduction of both solar panel area and battery mass, and, then, to satellite mass and cost reduction;

- ◆ better electromagnetic compatibility, allowing the operation of various equipments in small volumes;
- ◆ down link reduction, due to either data decimation or data pre-processing in earth observation applications, which allows both space segment and ground segment cost reduction, the latter being the key to enable direct-to-user data delivery services and to enlarge the user community;
- ◆ on board data processing allowing to supply real-time direct-to-user data delivery services to a large number of users.

All the considered integrated optical devices include acousto-optical (guided-wave Bragg cells) or other optoelectronic components (coupled charge device matrices, laser diodes, photodetectors), involving different effects. The modeling and design steps use a number of sophisticated CAD tools, based on different methods, including a complete original model of acousto-optic multi-frequency interaction in guided-wave multilayered structures [7]. Different fabrication technologies have been taken into account in the design step, including Ti-indiffusion and/or proton exchange (PE) in ferroelectric materials (above all lithium niobate, LiNbO_3), epitaxial growth of AlGaAs/GaAs-based multilayered structures and other III/V compounds. In this paper the potential of such devices is demonstrated by comparison with other electronic digital architectures.

Synthetic Aperture Radar

Fig. 1 shows the architecture of the optimized guided-wave optical processor for airborne real-time reconstruction of 2D images in side-looking SAR applications [8]:

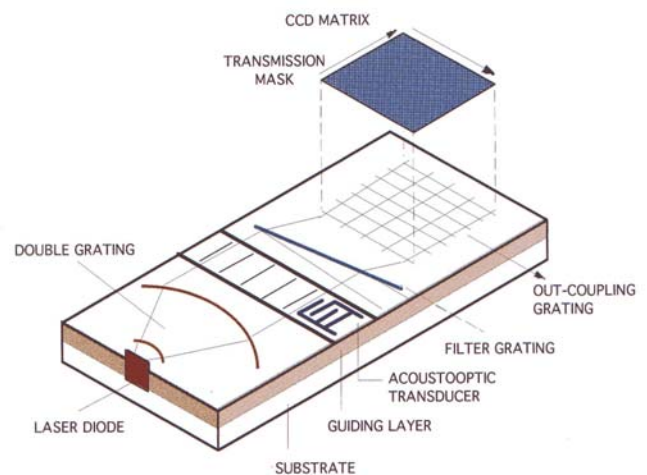


Figure 1 : Guided-wave AO approach to SAR

A laser diode is butt-coupled to a planar waveguide and emits TM-polarized light. Then, the laser beam is expanded and collimated by a double diffraction grating having non linear groove profiles. The second grating usually induces also a TE-polarized wave due to polarization conversion, since the planar waveguide usually supports both the polarizations. An acousto-optic Bragg cell deflects the incident optical beams by means of the interaction with the surface acoustic wave (SAW), generating at the output two diffracted (TM and TE) and two non diffracted (TM and TE) beams. The non diffracted beams are filtered by an appropriately designed reflection grating, the TM diffracted beam is coupled into a channel waveguide array by a Fresnel lens array, and the TE diffracted beam is off-axis deflected by the same lens array. Moreover, the TM beam is out-coupled by another grating and focused in order to uniformly illuminate a 2D coupled charge device (CCD) matrix. This illumination is modulated by a transmission mask, in close proximity to the CCD, which reproduces the azimuth reference chirp function of the transmitted SAR signal.

From the above description, the AO Bragg cell has a fundamental task in the processor, working for the SAR range data compression as a data correlator between the optical signal modulated by the laser diode and the acoustic signal modulated by IDT. The design of this component has been based on a very accurate and general model of acousto-optic interaction in guided-wave multilayered structures [9], where the SAW propagation is described in a matrix form [10] and each kind of material can be included in the structure, being characterized by its dielectric, piezoelectric and elastic tensors. The particular matrix formulation assures high stability and accuracy of the results.

Design criteria

One of the most important parameters in the design of such a kind of guided-wave processor is the length of the acoustic column, i.e. the collimation width of the optical guided beam, L_{beam} , along which the data correlation occurs. In fact, the processing time increases as long as the acoustic column, making possible images with better resolution or larger illuminated areas. To this aim, guided-wave structures having smaller SAW velocities $V_a(f)$ should be also important, where the frequency dispersion must be taken into account. However, the optical guided wave cannot be collimated over a width larger than about 1 cm, due to diffraction and fabrication tolerance limits. Then, the processing time is mainly influenced by the AO technology, ranging from about 2.85 μ s for Ti:LiNbO₃ waveguides (typically $V_a=3500$ m/s at 400

MHz for Y-cut, Z-propagating SAW) to 3.6 μ s for ZnO/AlGaAs/GaAs waveguides ($V_a = 2800$ m/s at 650 MHz for <110> (100) GaAs orientation). However, it is to be noted that a delay time of a few of microseconds for each range line is typical of any airborne SAR mission.

Therefore, if we consider a maximum and minimum range distance in the SAR illuminated range swath, the required processing time is given by $t_{delay} = 2(R_{max} - R_{min})/c$ and the acoustic column length is $L_{beam} = t_{delay} \cdot V_a(f_c)$, being c the light speed.

It is clear that the limit on L_{beam} , i.e. on t_{delay} , determines a limit on the maximum dimension of the swath range. It is also to be noted that the SAW velocity is, in general, a function of the IDT center frequency, which must be appropriately chosen. Moreover, the spectral separation of the correlation signal from other spurious components is assured at the output of the Bragg cell if the SAW is modulated by an appropriate frequency $f_R \geq 3B$, being B the IDT bandwidth. The theoretical range and azimuth resolutions depend on the SAR mission parameters. In fact, the range resolution is given by $\Delta X = c/2B$ and the azimuth resolution is $\Delta y = 2v_p / PRF$, where is the SAR platform speed and PRF the pulse repetition frequency. In the optical processing, where the CCD matrix has sizes $P \times Q$, the equivalent resolution of the optical processor becomes $\Delta x = L_{beam} / Q$.

The processor dynamic range, defined as the ratio of the strongest signal frame to the weakest signal frame that can be simultaneously detected, depends on the diffraction efficiencies of the device gratings and the output power of laser diode, according for the strongest permissible signal to

$$P_{det/pixel} = P_{laser} - \alpha L - \eta_{laser} - \eta_{double} - \eta_{Bragg} + \\ - \eta_{filter} - \eta_{lens} - \eta_{coupler} - \eta_{QE}$$

Assuming $P_{laser} = 15$ dBm, $\alpha = 0.5$ dB/cm (loss), $L = 2$ cm (total length), $\eta_{laser} = 5$ dBm, $\eta_{double} = 1$ dBm (80 %) , $\eta_{Bragg} = 13$ dBm (AO efficiency), $\eta_{lens} = 28.6$ dBm (70 %, 512 channels), $\eta_{coupler} = 1$ dBm (80 %), $\eta_{QE} = 5.2$ dBm (30 %), we should obtain $P_{det/pixel} = 15 - 54.8 = -39.8$ dBm. This means that the dynamic range becomes equal to 20.2 dB with a signal-to-noise ratio of one for a CCD matrix with a sensitivity of -60 dBm. A low AO efficiency (< 6%) is typically required for the correlation function linearity.

Details of design criteria for each guided-wave component of the integrated architecture can be found in the literature, including the acousto-optic Bragg cell [8-9].

A range delay time of the order of a few of μs , is compatible only with airborne applications, not spaceborne, where processing times longer than 200 μs are typically required. Therefore, the limit of the single processor is represented by the length of acousto-optic cell (about 1 cm), along which the fundamental range data compression occurs. This length depends on the sizes of the substrate crystal and the capability of collimating large optical beams. The solution for space-borne platforms consists in the use of a large number of optical processors working in parallel. Therefore, the SAR reference signal (chirp) should be applied to the Bragg cell of the first processor, travelling as an acoustic wave along that, and then going through another processor by another electrical transducer and so on up to the last one. The base-band received signal should be applied to the laser diode of each processor, and an appropriate electronic synchronization circuit should be used to perform the CCD column shifting for all the processors. This solution should allow the received data for longer time (hundreds of μs in space-borne applications) by using a number of identical processors.

Comparison with electronic approach

From a technological and overall performance point of view, the best architecture in airborne missions is demonstrated to be the monolithic Ti:LiNbO₃-based acousto-optic one, since the processor can be used to reconstruct the area of interest with good radiometric and geometric resolutions, reduced influence of speckle noise and scattering effects, in particular for perfectly separated point targets [11]. The approach is not particularly critical with respect to the illuminated area sizes or SAR mission data. Moreover, the Ti:LiNbO₃ is a very mature technology, widely used for a large number of integrated optical circuits for telecommunications, signal processing and computing. Therefore, the optical components of the circuit, including planar and channel optical waveguides, diffraction gratings, acousto-optic transducer and Fresnel lens array, can be fabricated in lithium niobate with high efficiency and low losses by using conventional fabrication techniques, such as electron beam lithography, reactive ion etching, thermal diffusion, RF sputtering.

Satellite SAR application

A number of processors are connected in parallel for the reconstruction of 2D SAR images from satellites. 800x800 CCD matrices, overall processing times of 230 μs for SAR platform height of 786 km, max antenna-target distance of 1000 km, SAR platform speed of 7562 m/s, PRF of 2 kHz, transmitted pulse bandwidth of 16 MHz have been assumed in the simulations. Both chirp and pseudo-random (PN)

signals have been used. Results are summarized in the next Table:

Table 1 : AO technologies for spaceborne SAR.

Acousto-Optic technology	PE:LiNbO ₃ Ti:LiNbO ₃ AlGaAs/GaAs
Integration level (all)	cell width \approx 1 cm
Number of parallel processors	90; 80; 68
Processing time of each cell	2.56; 2.86; 3.37 μs
Signal-to-noise ratio	10 dB (all)
Range resolution	< 30 m (all)
Azimuth resolution	\approx 30 m (all)
Radiometric resolution	3 dB (all)
Radiometric accuracy	3 dB (all)
Power consumption	10.8; 9.6; 68 W
Sizes	810; 504; 428 cm ³
Weight	9; 4; 3.4 kg
PN radiometric resolution	1 dB (all)
PN radiometric accuracy	< 1 dB (all)

While each technology will require real chirp signals and adaptive transmission masks to allow the reconfiguration of the system, the Ti:LiNbO₃ technology is the best choice to have low power consumption and technology maturity, but PE:LiNbO₃ should represent a good alternative, too. Although the guided-wave optical architectures cannot assure the high radiometric resolution and accuracy of the electronic processing, they are interesting and very compact alternatives for real-time onboard SAR processing.

Beam forming networks

Optical control techniques of microwaves have also been receiving good attention for many years. In fact, because of the compactness and high data parallelism allowed by the heterodyne mixing process, guided-wave optical architectures can generally permit reduced size, weight, power consumption and system complexity of the beam forming networks (BFNs) with respect to the MMIC-based electronic solutions. These advantages are particularly attractive for spaceborne applications, when the system hardware must be transferred onboard.

In Fig. 2 an optimized architecture of guided-wave AO processor [12] for beam forming and steering is shown. A TM-polarized laser beam is coupled to a Y-cut X-propagating Ti:LiNbO₃ waveguide. The beam is expanded and collimated by a double non linear grating. Then, two counter-propagating SAW Bragg cells deflect and frequency shift the TM wave coming from the gratings. At the output, a linear grating is used to filter the unwanted noise components of the diffracted beam, due to polarization conversion.

Finally, a linear photodetector array detects the deflected modes in the waveguide plane. Then, the photocurrent so generated for each array element is used to feed the corresponding BFN antenna element. By this approach, a continuous control of the BFN radiofrequency beam is allowed, by changing the frequency applied to the two IDTs.

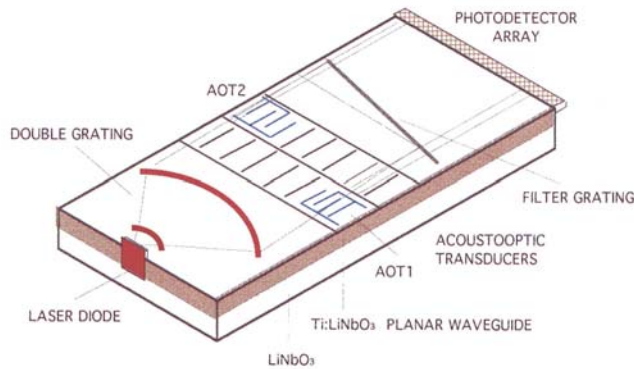


Figure 2 : Guided-wave AO processor for BFN

Table 2 shows a performance comparison between the optical and MMIC solutions. Advantages of the optical approach are obtained also in terms of phase errors for the antenna beam position.

Table 2 : Optical-electronic approach comparison.

Antenna elements	100 (optical)	96 (MMIC)
L-band frequency	800	< 1000 MHz
Switching rate	174 beams/ms	> 500 Mb/s
SNR ratio	> 10 dB	> 10 dB
Weight	100 g	> 1 kg
Power consumption	< 0.2 W	> 10 W
Chip size	600 mm ³	> 1000 mm ³
Beam positions	continuous	2 ¹⁶
Phase error (max)	≈ 2°	≈ 2°
Quan. phase error (max)	0	> 1°
Position beam error (max)	0.5°	> 1°
Mainlobe gain	≈ 14 dB	> 20 dB
Dynamic range	≈ 10 dB	> 10 dB

Conclusions

Some significant AO approaches for optical signal processing have been briefly reviewed. Comparisons between different technologies have been also summarized.

References

[1] J. Sapiel, D. Charissoux, V. Voloshinov, V. Molchanov, "Tunable acoustooptic filters and equalizers for WDM applications", *J. Lightwave Technol.*, vol. 20, pp. 892-899, 2002.

[2] P. Hee Su, S. Y. Kwang, H.Y. Seok, K. Y. Byoung, "All-fiber wavelength-tunable acoustooptic switches based on intermodal coupling in fibers", *J. Lightwave Technol.*, vol. 20, pp. 1864-1868, 2002.

[3] P. Maak, I. Frigyes, L. Jakab, I. Habermayer, M. Gyukics, P. Richter, "Realization of true-time delay lines based on acoustooptics", *J. Lightwave Technol.*, vol. 20, pp. 730-739, 2002.

[4] M.N. Armenise, V.M.N. Passaro et al., "Study on Innovative Opto-Electronic Applications Valuable for Space", ESA Contract n. RM/MTP/33096, 1997.

[5] M. N. Armenise, V.M.N. Passaro, M. Armenise, R. Diana, "Recent advances in guided-wave devices for optical signal processing", *Proc. of the Conf. on Optical Information Processing, Moscow, 28-31 May 1999*, vol. 3900, pp. 42-53, (INVITED PAPER).

[6] M.N. Armenise, V.M.N. Passaro, A.M. Matteo, M. Armenise, "On the performance limits of guided-wave devices for space applications", *Proc. of the Conf. on Photonics for Space Environments V, San Diego (CA), 1997*, vol. 3124, pp. 66-76.

[7] V.M.N. Passaro, A.M. Matteo, M.N. Armenise, "Modeling of Multifrequency Acoustooptic Interaction in Guided-Wave Bragg Cells", *IEEE J. Lightwave Technol.*, vol. 15, pp. 2114-2123, 1997.

[8] M.N. Armenise, F. Impagnatiello, V.M.N. Passaro, "Design and simulation of a GaAs acoustooptic correlator for real-time processing", *Optical Computing and Processing*, vol. 2, pp. 79-93, 1992.

[9] A.M. Matteo, V.M.N. Passaro, M.N. Armenise, "High-Performance Guided-Wave Acoustooptic Bragg Cells in LiNbO₃- and GaAs-based Structures", *IEEE Trans. on Ultrason., Ferroelectric and Fr. Control*, vol. 43, pp. 270-279, 1996.

[10] M.N. Armenise, V.M.N. Passaro, F. Impagnatiello, "Acoustic mode analysis of a homogeneous multilayer guiding structure", *OSA Journal Opt. Soc. Am. B*, vol. 8, pp. 443-448, 1991.

[11] V.M.N. Passaro, "Performance and simulation of an on-board guided-wave optical processor for airborne SAR applications", *Optical and Quantum Electronics*, vol. 34, pp. 893-913, 2002.

[12] M.N. Armenise, V.M.N. Passaro and G. Noviello, "Lithium niobate guide-wave beam-former for sheering phased array antennas", *Applied Optics*, vol. 33, pp. 6194-6209, 1994.